

Two-photon excitation with pico-second fluorescence lifetime imaging to detect nuclear association of flavanols

Irene Mueller-Harvey ^{a,*}, Walter Feucht ^b, Juergen Polster ^c, Lucie Trnková ^d, Pierre Burgos ^e, Anthony W. Parker ^e, Stanley W. Botchway ^e

^a *Chemistry & Biochemistry Laboratory, Food Production & Quality Research Division, School of Agriculture, Policy & Development, University of Reading, P O Box 236, Reading RG6 6AT, UK*

^b *Department of Plant Sciences, Technical University of Munich (TUM)*

Wissenschaftszentrum Weihenstephan (WZW), D-85354 Freising, Germany

³ *Department of Physical Biochemistry, Technical University of Munich (TUM), Wissenschaftszentrum Weihenstephan (WZW), D-85354 Freising, Germany*

⁴ *University of Hradec Králové, Faculty of Science, Department of Chemistry, Rokitanského 62, 50003 Hradec Králové, Czech Republic*

⁵ *Central Laser Facility, Research Complex at Harwell, Science and Technology Facilities Council, Rutherford Appleton Laboratory, Harwell - Oxford, Didcot, OX11 0QX, UK*

Corresponding author. Tel.: +44 (0)118 378 6619; fax: +44 (0)118 935 2421.

E-mail address: i.mueller-harvey@reading.ac.uk;

E-mail addresses of co-authors:

Walter Feucht: walter.feucht@gmail.com

Juergen Polster: j.polster@wzw.tum.de

Lucie Trnková: lucie.trnkova@uhk.cz

Pierre Burgos: pierre.burgos@stfc.ac.uk

Anthony W. Parker: tony.parker@stfc.ac.uk

Stanley W. Botchway: stan.botchway@stfc.ac.uk

Keywords: Fluorescence lifetime imaging microscopy, flavanols, epigallocatechin gallate, nuclear binding, histone proteins, multiphoton excitation.

Two-photon excitation with pico-second fluorescence lifetime imaging to detect nuclear association of flavanols

1

2 Irene Mueller-Harvey ^{a,*}, Walter Feucht ^b, Juergen Polster ^c, Lucie Trnková ^d, Pierre Burgos
3 ^e, Anthony W. Parker ^e, Stanley W. Botchway ^e

4

5 ^a *Chemistry & Biochemistry Laboratory, Food Production & Quality Research Division,*

6 *School of Agriculture, Policy & Development, University of Reading, P O Box 236,*

7 *Reading RG6 6AT, UK*

8 ^b *Department of Plant Sciences, Technical University of Munich (TUM),*

9 *Wissenschaftszentrum Weihenstephan (WZW), D-85354 Freising, Germany*

10 ^c *Department of Physical Biochemistry, Technical University of Munich (TUM),*

11 *Wissenschaftszentrum Weihenstephan (WZW), D-85354 Freising, Germany*

12 ^d *University of Hradec Králové, Faculty of Science, Department of Chemistry,*

13 *Rokitanského 62, 50003 Hradec Králové, Czech Republic*

14 ^e *Central Laser Facility, Research Complex at Harwell, Science and Technology Facilities*

15 *Council, Rutherford Appleton Laboratory, Harwell - Oxford, Didcot, Oxfordshire, OX11*

16 *0QX, UK*

17

18 **ABSTRACT**

19 Two-photon excitation enabled for the first time the observation and measurement of

20 excited state fluorescence lifetimes from three flavanols in solution, which were ~ 1.0 ns

21 for catechin and epicatechin, but <45 ps for epigallocatechin gallate (EGCG). The shorter

22 lifetime for EGCG is in line with a lower fluorescence quantum yield of 0.003 compared to
23 catechin (0.015) and epicatechin (0.018).

24

25 *In vivo* experiments with onion cells demonstrated that tryptophan and quercetin, which
26 tend to be major contributors of background fluorescence in plant cells, have sufficiently
27 low cross sections for two-photon excitation at 630 nm and therefore do not interfere with
28 detection of externally added or endogenous flavanols in *Allium cepa* or *Taxus baccata*
29 cells. Applying two-photon excitation to flavanols enabled 3-D fluorescence lifetime
30 imaging microscopy and showed that added EGCG penetrated the whole nucleus of onion
31 cells. Interestingly, EGCG and catechin showed different lifetime behaviour when bound to
32 the nucleus: EGCG lifetime increased from <45 to 200 ps, whilst catechin lifetime
33 decreased from 1.0 ns to 500 ps. Semi-quantitative measurements revealed that the relative
34 ratios of EGCG concentrations in nucleoli associated vesicles : nucleus : cytoplasm were
35 *ca.* 100:10:1.

36

37 Solution experiments with catechin, epicatechin and histone proteins provided preliminary
38 evidence, via the appearance of a second lifetime ($\tau_2 = 1.9$ to 3.1 ns), that both flavanols
39 may be interacting with histone proteins. We conclude that there is significant nuclear
40 absorption of flavanols. This advanced imaging using two-photon excitation and
41 biophysical techniques described here will prove valuable for probing the intracellular
42 trafficking and functions of flavanols, such as EGCG, which is the major flavanol of green
43 tea.

44

45 *Keywords:* Fluorescence lifetime imaging microscopy, flavanols, epigallocatechin gallate,
46 nuclear association, histone proteins, multiphoton.

47

48 **1. Introduction**

49 Plants synthesise >4000 different flavonoid compounds, which can be grouped into several
50 different subgroups. Flavanols (Fig. 1) are an important subgroup that is widespread in
51 plants and plant foods [1]; they are also precursors of condensed tannins, which are the
52 fourth largest group of natural plant products after cellulose, hemicellulose, and lignin [2].
53 These polyphenolic compounds are attracting considerable interest, because diets rich in
54 fruits and vegetables are associated with improved health and a reduction of age-related
55 diseases such as cancer, osteoporosis and cardiovascular diseases [3-7]. Flavonoids are
56 considered to be ‘lifespan essentials’ and recent reviews suggest that their antioxidant
57 properties alone are unlikely to explain their beneficial effects on human health or their
58 functions in plants [8-10].

59

60 A consensus is emerging that *in vitro* and *in vivo* experiments need to probe the
61 bioavailability of these polyphenols and their molecular targets [3,6,8,10-11]. *In vitro*
62 studies have tended to require 10 to 100-fold higher polyphenol concentrations than are
63 usually found in mammalian plasma and tissues in order to achieve many of the reported
64 medicinal effects [5,12]. However, the existence of high-affinity targets for dietary
65 polyphenols might explain their health-promoting effects and in this context it is pertinent
66 to examine more closely recent evidence that nuclei from both plant *and* mammalian cells
67 acted as sinks for flavanols [13-17]. Although the function of these secondary plant

68 metabolites requires further elucidation, evidence is emerging that they may be important in
69 cell development. For example, loss of flavanols has been linked to defective pollen
70 development [14]. Different types of flavanol distribution patterns were observed in *Tsuga*
71 *canadensis* at the sub-nuclear level [13] and the authors questioned whether the epigenetic
72 code of histones could affect flavanol-chromatin associations. Moreover, Feucht *et al.* [15]
73 found identical flavanol patterns within different cell lineages in a meristematic plant tissue
74 and suggested that this could be indicative of a synchronized, transcriptional regulation. In
75 addition, nuclear flavanol concentrations clearly depended on the season, i.e. during
76 dormancy they were almost absent but during growth periods relatively high amounts were
77 observed [18]. The fact that flavanols were associated with both interphase and mitotic
78 chromosome states posed the question of whether flavanols might be associated with
79 histones. If this is the case, then this could open a new perspective on genomic regulation.

80

81 This research by Feucht's group made use of the fact that flavanols form a blue
82 condensation product with dimethylaminocinnamaldehyde (DMACA) [19]. The DMACA
83 reagent is, however, a relatively aggressive reagent that requires 0.75 M sulfuric acid for
84 the staining reaction and this could cause some physical damage within the cells. Polster *et*
85 *al.* [18], therefore, tested the existence of nucleus-bound flavanols with a milder technique,
86 i.e. laser microdissection and pressure catapulting (LMPC), which separated intact nuclei
87 from cells and these also stained blue in the subsequent DMACA reaction. Nevertheless,
88 LMPC causes physical rupture of the cytoplasm that surrounds the nuclei and could have
89 given rise to an artificial DMACA reaction. Moreover, histological studies with DMACA
90 cannot distinguish between different flavanols or between flavanol monomers, oligomers or

91 polymers [19]. Techniques are therefore required that can establish the sub-cellular
92 localisation, and concentrations therein, of flavanols to probe their functionality and
93 metabolism in plant and mammalian cells.
94
95 Nifli *et al.* [29] recently applied confocal fluorescence microscopy to map the intracellular
96 distribution of a major plant flavonol, i.e. quercetin (Fig. 1), which has a UV absorption
97 λ_{max} of 372 nm. Quercetin revealed a specific fluorescence (488 nm_{ex}/500-540 nm_{em}) in the
98 cellular environment at physiologically relevant concentrations (<5 μM), which the authors
99 attributed to non-covalent binding to cellular components. Intracellular tracing of flavanols
100 ($\lambda_{\text{max}} \sim 280$ nm; Fig. 1 and Fig. S1) by UV-Vis spectroscopy or confocal fluorescence
101 microscopy is, however, not possible because plant and mammalian cells contain numerous
102 compounds which would interfere with the detection of flavanols by giving background
103 fluorescence signals (termed “auto-fluorescence”). Fig. 2 illustrates the photophysical
104 processes in a conventional Jablonski diagramme, which depicts one- and two-photon
105 excitation and various relaxation pathways that are open to the electronic excited state
106 following photon(s) absorption.

107

108 In fluorescence life-time imaging microscopy (FLIM) both fluorescence intensities and
109 fluorescence lifetimes of specific compounds can be measured at each pixel in the image
110 [21,22]. In addition, variations in fluorescence lifetime can provide further image contrast:
111 lifetime shifts can serve as sensitive probes for detecting molecular interactions and may
112 yield information on a compound’s environment, such as pH or oxygen concentration [23-
113 25]. Lifetime, τ , is derived from the time-constant of the fluorescence decay (Fig. 2), where

114 $\tau = 1/k_{\text{fluorescence}}$. FLIM is based on either single- or multi-photon excitation techniques.
115 Multi-photon excitation with femtosecond lasers offers many advantages for biological
116 measurements over more conventional single photon excitation [23,26]:

- 117 ✓ Excitation with red light that is not directly absorbed by cellular materials.
- 118 ✓ Reduced cellular toxicity in biological studies.
- 119 ✓ Reduced photo-bleaching.
- 120 ✓ Deeper penetration of the near-infrared light into the biological specimen.
- 121 ✓ Femtolitre volume excitation.
- 122 ✓ A flexible imaging platform that is capable of resolving several (and related)
123 compounds.
- 124 ✓ The ability to deliver UV-equivalent photon energies directly beneath UV absorbing
125 materials and molecules.
- 126 ✓ An ability to perform time-resolved studies due to the short pulsed light source.

127 In two-photon excitation (2PE) the simultaneous absorption of two lower energy photons
128 mimics the absorption of a single photon of equivalent higher energy (Fig. 2). Thus, 2PE at
129 560 nm mimics UV excitation at 280 nm [23,27]. In FLIM ultrafast lasers providing pulse
130 lengths of the order of 200 femtoseconds (200×10^{-15} s) enable time-resolved
131 measurements, which can detect molecular interactions in solution and cells [23-25,28] and
132 can be used to construct fluorescence life-time maps of a compound's distribution within
133 viable cells.
134

135 Here we describe 2PE experiments designed to eliminate any doubts regarding the results
136 from previous histological studies that employed the DMACA staining reagent. Two-
137 photon excitation coupled to 3-D fluorescence lifetime imaging microscopy enabled
138 examination of intact biological tissues and highly localised, non-destructive and selective
139 detection of flavanols. The fluorescence behaviour of three flavanols, catechin, epicatechin
140 and epigallocatechin gallate (EGCG) (Fig. 1), was measured first in model solution systems
141 and then in two natural cell systems, onion epidermis cells and *Taxus* pollen mother cells.
142 These flavanols were chosen because they are widespread in plants and are also
143 bioavailable and bioactive in several *in vitro* and *in vivo* mammalian cell systems
144 [1,6,9,29]. Solution phase studies were first used to optimise and measure spectroscopic
145 shifts and lifetime changes of free flavanols *versus* flavanols bound to DNA or histone
146 proteins at normal physiological pH values. The optimised spectroscopic parameters were
147 then applied to probe the intra-cellular location of externally added flavanols in *Allium cepa*
148 cells and of endogenous flavanols in *Taxus baccata* cells. The same plant models had been
149 tested previously with the DMACA staining reagent [14,30].

150

151 **2. Methods and materials**

152 *2.1. Reagents*

153 The following reagents were purchased from Sigma-Aldrich Company Ltd, UK:
154 (+)-catechin (98%), (-)-epicatechin (90%), (-)-epigallocatechin gallate (95%; EGCG), tris-
155 (hydroxymethyl)amino methane (Tris), K₂HPO₄ (ACS reagent, (≥ 98%), KH₂PO₄ (ACS
156 reagent, (≥ 99%), DNA from calf thymus and Histone type II-A. Histone was supplied by
157 Roche Diagnostics Ltd, UK. Histone sulphate from calf thymus was purchased from Fluka

158 (Sigma-Aldrich Chemie, Steinheim, Germany; Polster *et al.*, 2003). Ethanol (LiChrosolv, ≥
159 99.9%) was purchased from VWR-Merck, UK.

160

161 Tris buffers (0.1 M) were prepared and adjusted to pH 7.0 and 8.0 with HCl and phosphate
162 buffers (0.1 M) at pH 5.8, 7.1 and 8.2 were prepared using K₂HPO₄ and KH₂PO₄ as
163 described [16].

164

165 2.2. Calculation of relative fluorescence quantum yields of the flavanols

166 Flavanols were dissolved in methanol to yield 0.01 M stock solutions. Subsequent dilutions
167 for 20 and 40 μM flavanol concentrations were made with sodium phosphate buffer (pH
168 7.4, 0.1 M, 0.05% sodium azide). These were placed in a 10 mm quartz Suprasil
169 fluorescence cuvette (Hellma, Germany) and UV-Vis spectra were first recorded from 190
170 to 500 nm using a Helios β spectrophotometer (Spectronic Unicam, U.K.). Then
171 fluorescence spectra were recorded using a luminescence LS-55 spectrometer (Perkin
172 Elmer, U.K.) from 290 to 530 nm with excitation at 295 nm under continuous stirring. The
173 excitation and emission slits were both set to 5 nm and scanning speed was 200 nm min⁻¹.
174 All experiments were carried out at 37 °C. The literature reported a quantum yield of 0.12
175 for tryptophan (Trp) at 270 nm (website) and we confirmed this for 295 nm. Therefore, the
176 quantum yields of flavanols (Flav) were calculated relative to tryptophan using the
177 integrated area between 300 and 530 nm under the fluorescence spectra [31-33] according
178 to:

179
$$\text{Absorption at 295 nm (Trp)} * 0.12 * \text{Fluorescence (Flav)}$$

180
$$\text{Quantum yield}_{(\text{Flav})} = \frac{\text{Absorption at 295 nm (Trp)} * 0.12 * \text{Fluorescence (Flav)}}{\text{Absorption at 295 nm (Flav)} * \text{Fluorescence (Trp)}}$$

181 Absorption at 295 nm (Flav) * 0.12 * Fluorescence (Trp)

182

183 2.3. Flavanol solutions

184 Flavanols were dissolved in ethanol (~10 mM) and prepared fresh on a daily basis. Just
185 before measuring the fluorescence lifetimes, aliquots (10 µL) were removed and diluted
186 with buffer, DNA or histone protein solutions (90 and 40 µL) to obtain flavanol
187 concentrations between 1 and 2 mM.

188

189 DNA (0.6 mg) was dissolved in Tris buffer (pH 8.0; 30 mL) overnight at 4 °C. Sigma
190 histone (5.9 mg) was dissolved in Tris buffer (pH 7.0 and 8.0; 2.85 mL). Ethanol (98 µL)
191 was added to the pH 8.0 buffer to facilitate dissolution. Histone sulphate (0.8 mg) was
192 dissolved in Tris buffer (pH 7.0 and 8.0) according to Polster *et al.* [16]. The supernatants
193 were used after centrifugation. Roche histone (1.0 mg) was dissolved in Tris buffer (pH 7.0
194 and 8.0; 500 µL) and ethanol (10 µL).

195

196 2.4. Plant samples

197 The thin adaxial epidermis from onion (*Allium cepa*) bulb scale was removed, cut into 2
198 cm² pieces and incubated with aqueous catechin or EGCG solutions (1 mM; 20 mL) for up
199 to 8 h [30].

200

201 Male cones from yew (*Taxus baccata*) were harvested on 5th October 2008. The eight cover
202 leaves were removed and the yellow anthers were gently squeezed with tweezers in order to
203 release the mother pollen cells. Preliminary experiments revealed that these cells stained

204 dark blue with the DMACA reagent (10 mg DMACA dissolved in 1 mL of 0.75 M H₂SO₄)
205 [30].

206

207 *2.5. Multiphoton microscopy*

208 The set up used in this study has been previously described [23]. Briefly, a custom built
209 two-photon microscope was constructed using scanning XY galvanometers (GSI Lumonics
210 Ltd). A diode-pumped (Verdi V18) titanium sapphire (Mira F900) operating at 700-980 nm
211 generated laser light at a wavelength of 585 ± 2 nm and was used for the solution studies
212 and at 630 ± 2 nm for the plant cell studies through an optical parametric oscillator (OPO,
213 APE-Coherent GmbH, Berlin, Germany) operating at 180 fs pulses at 75 MHz. The pulse
214 width was maintained using a femto control unit (APE Coherent GmbH). The laser beam
215 was focused to a diffraction-limited spot using a water-immersion ultraviolet corrected
216 objective (Nikon VC x60, NA 1.2) and specimens were illuminated at the microscope stage
217 of a modified Nikon TE2000-U with UV transmitting optics. Fluorescence emission was
218 collected without descanning, bypassing the scanning system, and passed through a $340 \pm$
219 20 nm interference filter (U340, Comar Instruments, Cambridge, UK). Emission
220 fluorescence was detected using an external fast microchannel plate photomultiplier tube
221 (Hamamatus R3809U-50) and recorded using a Time-Correlated Single Photon Counting
222 (TCSPC) PC module SPC830 (Becker and Hickl GmbH, Berlin, Germany). Fluorescence
223 lifetime image microscopy was performed by synchronising the XY galvanometer positions
224 with the fluorescence decay. The X,Y galvanometers were raster scanned at 1 ms or 2 ms
225 per pixel for 128 x 128 or 256 x 256 image size, respectively, giving a 33 sec per image

226 frame. The presented images were three accumulations to allow for enough photon counts
227 per channel for the data analysis.

228

229 2.6. *Image analysis*

230 Steady state grey scale images (8 bit, up to 256 x 256 pixels) are produced by binning all
231 decay photons as a single channel. Fluorescence lifetime images were obtained for control
232 cells and flavanol-loaded cells by analysing the decay at individual pixels using a single or
233 double exponential curve fitting (SPCImage 2.94 analysis software Becker and Hickl). A
234 thresholding function within the FLIM analysis software ensured that noncorrelating
235 photons leading to background noise arriving at the detector were not included in the
236 analysis. Single point decay analysis was carried out without binning while FLIM was
237 analysed with a maximum of 2 binning.

238

239 **3. Results and discussion**

240 3.1. *Flavanol fluorescence lifetimes in aqueous solutions*

241 It is well known that flavanols oxidise readily in alkaline pH [4], therefore lifetimes were
242 first examined at pH values ranging from 5.8 - 8.2. Fig. 3 shows that the fluorescence
243 lifetime, τ , of catechin (2 mM catechin solution in 0.1 M phosphate buffer) was relatively
244 stable between pH 5.8 and 7.1: τ was 1.0 ns at the start and 0.9 ns after 20 min. However, at
245 pH 8.2 the lifetime changed from 1.0 to 0.7 ns within 20 minutes. When the same
246 measurements were conducted under a nitrogen blanket, lifetime reduction was kept to 9%
247 over a 30 min period and this agrees with Sang *et al.* [34] who found that flavanols were
248 not oxidised under nitrogen. Therefore, all subsequent solution measurements were

249 determined immediately after mixing the solutions, i.e. within 30 seconds. Fig. 3 also
250 shows that pH *per se* had no effect on catechin lifetimes: τ of catechin was ~ 1.0 ns at pH
251 5.8, 7.1 and 8.2. The reduction in τ values can also not be ascribed to sample concentration
252 or the presence of non-interacting or energy transfer products, as the excited state lifetime
253 is independent of both of these.

254

255 The natural lifetime of catechin in solution in the absence of oxygen is ~ 1.1 ns (Fig. 3).
256 This reduces, via quenching, as expected in the presence of dissolved oxygen ($7.6 \text{ mg}\cdot\text{L}^{-1}$)
257 at room temperature and pressure to ~ 1 ns. It is worth noting that at high oxygen
258 concentrations, 30 mM, the quenched lifetime observed will be as expected taking into
259 account diffusion control rate. Therefore the subsequent change in lifetime (Fig. 3) (to ~ 0.7
260 ns after 20 min in oxygen) is very likely due to the formation of a deprotonated or oxidised
261 product as the OH groups in the B-ring are particularly susceptible to deprotonation and
262 therefore oxidation at alkaline pH [35]. It is interesting to note that the reduced lifetime
263 fitted well to a single exponential decay, again indicating a single fluorescent molecular
264 species is present and favouring the observed decreases in lifetime results from either a
265 photoproduct, which also fluoresces, or an oxygen quenched process. Further studies using
266 high performance liquid chromatography may help identify these oxidised products.

267

268 Importantly, Fig. 4 shows that flavanols had different fluorescent decay curves.

269 Fluorescence lifetimes of catechin and epicatechin were similar (1.0 and 1.1 ns,

270 respectively). However, in the case of EGCG at pH 8.1 (2 mM flavanol solutions in 0.1 M

271 phosphate buffer) the lifetime was found to be within the instrument response function and
272 Fig. 4 shows only the characteristics of the fast micro-channel plate (<45 ps). Ultrafast time-
273 resolved Kerr gated fluorescence spectroscopy will be needed to resolve the EGCG lifetime
274 in the future. EGCG differs from catechin and epicatechin by the presence of a galloyl
275 group at C-3 (Fig. 1). The lifetime of the excited state is given by the sum of the different
276 competing relaxation processes, which include fluorescence, non-radiative decay,
277 intersystem crossing and chemical reaction as illustrated in Fig. 2. The shorter lifetime for
278 EGCG is most likely due to the presence of additional phenolic groups, which would be
279 expected to enhance the solvation effects and which in turn would influence the non-
280 radiative decay processes. These extra phenolic groups also enhance its antioxidant
281 properties [36] and this presumably makes it more susceptible to oxidation. Indeed, the
282 fluorescence quantum yield of EGCG is much lower than that of catechin or epicatechin
283 (Table 1) suggesting that the non-radiative rate (k_{IVR} ; Fig. 2) dominates in the relaxation of
284 the electronic excited state.

285

286 At pH 8, epicatechin also had a two-component fluorescence decay lifetime (see footnote in
287 Supplementary Table). The exact physical origin of the bi-exponential lifetime is unknown.
288 However, it is not uncommon for fluorophores in complex cellular environments to
289 demonstrate multiple decay times as seen in Table 2. Different decay times represent
290 differing physical influences that the nascent electronic excited states are subjected to and
291 consequently may lead to differences in the efficiency of the energy loss process and return
292 to the ground state. The fact that we see a bi-exponential decay indicates that the flavanols
293 find themselves in two differing states and/or two different environments; for example free

294 and bound forms (Supplementary Table). Further investigations studying the ultrafast
295 dynamics will be needed to help explain these differences and/or whether diastereoisomers
296 such as catechin and epicatechin have different fluorescence properties.

297

298 *3.2. Fluorescence lifetime imaging microscopy*

299 *3.2.1. Control experiments with onion cells*

300 The experimental conditions developed above for flavanol solutions were applied initially
301 to onion root cells (tissue soaked in water for 5 h; and followed by two-photon excitation at
302 585 nm). Lifetime decay curves, at several different points in the cells, could be fitted to a
303 single exponential decay giving a τ value between 2.3 and 2.6 ns ($\chi^2 = 1.05$). It is highly
304 likely, however, that under these excitation conditions the emission and lifetime values are
305 mainly due to auto-fluorescence contributions from tryptophan [23]. In order to avoid
306 significant background fluorescence signals from other cellular materials, in particular
307 aromatic amino acids, e.g. tryptophan, when using UV excitation at 290 nm (equivalent to
308 580 nm 2PE excitation) the 2PE excitation wavelength was shifted to 630 nm, which has
309 been shown to give little background interference [23]. Control experiments were then
310 carried out without added flavanols, i.e. in the presence of just water, in order to
311 substantiate that the fluorescence was due to flavanols. The onion sample without added
312 flavanol showed only weak auto-fluorescence and a τ value of 0.8 ns ($\chi^2 = 1.60$) (Fig. 5c)
313 confirming that our FLIM measurements were tracking the flavanol presence in cells (see
314 Section 3.2.2. below). Whole onions are known for their high quercetin concentration (Fig.
315 1) [6], but given the low photon count, we can conclude that neither tryptophan nor

316 quercetin interfered with flavanol detection, λ_{em} , at 340 ± 20 nm if 2PE with λ_{ex} was 630
317 nm.

318

319 3.2.2. Absorption of flavanols by onion nuclei

320 Fig. 5a and 5b show fluorescence lifetime maps of cells in an onion epidermis, which had
321 been soaked in 1 mM aqueous flavanol solutions. Following absorption of catechin or
322 EGCG, the fluorescing nuclei and several bright, small spots of ~ 2 to $7 \mu\text{m}$ were clearly
323 visible to a much greater extent than the surrounding cell matrix. Careful analysis of Fig. 5b
324 showed a bright spot of $4 \mu\text{m}$ diameter. It is known that inactive nuclei possess very small
325 nucleoli of the order of $\sim 1 \mu\text{m}$ [37]. The observed spot is too large to be a nucleolus, we
326 therefore propose that the bright spot was a clustering of perinucleolar organiser regions
327 (NORs) [38]. NORs tend to surround the nucleoli and strongly absorb flavanols [13].

328

329 This study demonstrated that FLIM combined with 2PE at 630 nm enabled *in vivo*
330 detection of both catechin and EGCG and avoided interference by tryptophan or quercetin,
331 as the control showed hardly any fluorescence (Fig. 5c). We have previously shown that
332 there is negligible excitation of cellular auto-fluorescence, particular from tryptophan,
333 following multiphoton excitation at 630 nm [23]. Although tryptophan may be excited by
334 multi-photon treatment at 590 nm, which is equivalent to single photon excitation (1PE) at
335 295 nm, this diminishes by a factor of 10 at 630 nm. Furthermore, the excited state lifetime
336 of tryptophan (~ 3 ns) is significantly different to that of the flavanols investigated here.
337 These findings, therefore, provided clear and unequivocal evidence for nuclear flavanol
338 absorption. Since the excited state lifetime may be influenced by the environment of the

339 flavanols, the colour trend seen in the FLIM images (Fig. 5a,b) may be due to slight
340 differences in the environment of the absorbed flavanols. A series of z axis images taken
341 through a cell revealed that EGCG was detectable throughout the nucleus and not just at the
342 surface (Video Clip S1). EGCG appeared to be concentrated in the NORs; relative
343 proportion of EGCG photon counts were 1 to 3 (cytoplasm) : 10 (nucleus) : 100 to 150
344 (NORs) (*data not shown*).

345

346 3.3. FLIM lifetimes of bound versus free flavanols in solution

347 Fluorescence decay curves of nucleus-bound catechin were best fitted to two components,
348 i.e. $\tau_1 = 0.5$ ns (77.5%) and $\tau_2 = 2.7$ ns (22.5%; χ^2 of 1.04) (Table 2). It is unlikely that τ_2
349 emanates from tryptophan as the same experiments with EGCG fitted to a single
350 component decay with an average τ of 0.25 ± 0.05 ns (Table 2). The increase in EGCG
351 lifetime from <0.045 ns in solution (Fig. 4) to 0.25 ns in the nucleus is a reverse of the
352 trend seen for catechin, which showed a lifetime of ~ 1 ns in solution and 0.5 ns in the
353 nucleus.

354

355 The effect of nuclear association generating different lifetimes is given in Table 2 and was
356 recorded when Fig. 5 was taken. Taken together, these observations suggest that the two
357 flavanols (catechin and EGCG) may differ in their interaction mechanisms with nuclear
358 components. The lowering of a lifetime indicates either an enhanced non-radiative decay
359 (through for example formation of hydrogen bonds) [31] or possibly self-association which
360 has been reported for catechin [39]. A decrease in lifetimes upon cellular absorption has
361 also been reported for 5-hydroxytryptophan and was attributed to self-quenching or

362 environmental effects [23]. Further research will be needed to establish whether oxidation
363 during the cellular absorption experiment could have contributed to the shorter catechin
364 lifetime (Fig. 3) and whether oxidation would have increased EGCG fluorescence lifetime.
365 It seems, however, more likely that this contrasting lifetime behaviour is indicative of
366 different interaction mechanisms.

367

368 *3.4. Endogenous flavanols in Taxus baccata*

369 The same 2PE experimental conditions were then applied to pollen mother cells which had
370 been isolated from microspores of male *Taxus baccata* cones. According to Feucht *et al.*
371 [14] late tetrads and early microspores possess endogenous catechin and epicatechin. We
372 observed, however, fluorescence lifetimes, which could be fitted to single component
373 decays with τ of 0.2 ns and which resembled EGCG, rather than catechin or epicatechin
374 (Table 2). Interestingly, the photon count of the signal to noise ratio from endogenous
375 flavanols in the *Taxus* cells was not dis-similar to onion cells soaked in a 1 mM EGCG
376 solution. Younger cones at the tip of the *Taxus baccata* twig yielded twice as many photons
377 compared to slightly more mature cones from further along the twig. This finding agrees
378 with previous observations [14,15] that nuclear DMACA staining for flavanols was most
379 intense during high cell activity, e.g. in mitotic and stem cells. Interestingly, it also
380 coincides with observations of higher EGCG concentrations in foetal than maternal plasma
381 of rats: absorbed catechins were found in the brain, eye, heart, lung, kidney, liver and
382 placenta of fetal organs [40].

383

384 *3.5. Flavanol fluorescence lifetimes in the presence of DNA or histone proteins*

385 The fact that flavanols bind to the nucleus raises an important question: which nuclear
386 components act as the binding sites? Several previous studies demonstrated that DNA
387 interacts with planar flavonoids, such as flavonols and anthocyanidins, and depending on
388 the experimental conditions, these interactions were either weak or led to intercalation [41].
389 However, flavanols are *not* planar and may therefore not be able to intercalate with DNA.
390 We, therefore, explored fluorescence lifetime behaviour of flavanols in the presence of
391 DNA. Addition of DNA had no effect on catechin or epicatechin lifetimes in aqueous
392 solutions (2 mM; pH 8 in Tris buffer; data not shown). This agrees with results from UV-
393 Vis spectroscopic titrations which also found that DNA did not interact with catechin or
394 EGCG in 0.1 M Tris at pH 7.4 or 8.0 [16].

395

396 However, Polster *et al.* [16] reported that histone proteins might be the nuclear targets for
397 catechin and EGCG. Using UV-Vis titration experiments, they showed that both flavanols
398 bound to histone sulphate and interactions were more pronounced at pH 8.0 than 7.4 in Tris
399 buffer. Since these titration experiments required approximately 1 h in total [42], it could be
400 argued that this might be sufficient time for oxidative reactions and artefact formation to
401 occur especially at higher pH values as determined in Fig. 3. The present fluorescence
402 lifetime measurements were, however, made within 30 s of mixing the flavanol and histone
403 solutions (note: the fluorescence lifetime experiments were also done in Tris buffer, as the
404 UV-Vis titrations revealed that histone sulphate showed a less pronounced interaction with
405 catechin in phosphate than Tris buffer [16]).

406

407 The lifetimes of catechin and epicatechin in the presence of histone proteins were
408 investigated at two concentrations (1.1 and 1.9 mM) and pH (7 and 8) (Supplementary
409 Table). Given the short lifetimes recorded and the errors in fitting bi-exponential decays,
410 the data for the different flavanols need careful interpretation. At this stage we are unable to
411 clearly identify whether or not histones bind to flavanols, which would be expected to be
412 shown by a change in lifetime (i.e. due to quenching). From other work it is, however, also
413 clear that histone preparations differ in their ability to associate with flavanols [13] and,
414 therefore, further fluorescence studies will be needed. Nevertheless, these initial findings
415 demonstrate the potential power of studying flavanol–histone interactions by fluorescence
416 methods. It is now also evident that much fundamental work is needed for characterising
417 how the chemical environment (including pH and oxygen concentration) influence
418 fluorescence lifetimes, quantum yields and spectra of flavanols. With regard to pH, the pK_a
419 values of catechin, for example, are *ca.* 8.6 and 9.4 [43] and thus at pH 8 three different
420 protolyte species exist for catechin: BH_2 , BH^- , and B^{2-} . The fluorescence behaviour of each
421 of these species will need to be understood and only through such careful measurements
422 can these types of fluorescence measurements provide the much needed tool for elucidating
423 the interactions between flavanols, histones and DNA.

424

425 *3.6. Possible role of nuclear flavanols beyond an antioxidant function*

426 Nuclear absorption has been reported not only for flavanols [13] but also for some other
427 flavonoids. *Arabidopsis thaliana* nuclei absorb flavonols [44,45], *Drosophila* follicle nuclei
428 absorb quercetin [46] and *Flaveria chloraefolia* nuclei absorb sulfonated flavanols [47]. It
429 used to be widely accepted that the major function of polyphenols such as flavonoids was

430 to protect DNA against UV damage and oxidative stress, but this has now been questioned
431 [8,10]. Instead they were shown recently also to affect cell signalling and gene expression
432 [48,49]. Flavanols are involved in the transcriptional activation of genes and modulation of
433 epigenetic changes [36,50].

434

435 Whilst several dietary flavonols and the green tea flavanol, EGCG, have been implicated in
436 interacting and protecting DNA against damage [41,51, 52], the fact that they inhibit DNA
437 methyltransferases *in vitro* and *in vivo* at the μ molar to sub- μ molar level is potentially more
438 important for their effects on health [5,7,29,48,53]. Moreover, EGCG was also a potent
439 inhibitor of histone acetyltransferase [50]. Histone acetylation has previously been shown
440 to affect flavanol association [13,16] and is known to alter the chromatin structure, which in
441 turn has been linked to the transcriptional activation of genes [15]. Both processes, DNA
442 methylation and histone acetylation, are involved in epigenetic changes [54]. Indeed,
443 Yamada *et al.* [53] concluded that EGCG may have inhibitory effects on the epigenetic
444 changes that occur during carcinogenesis and aging. Whilst we found no evidence for
445 interactions between flavanols and DNA, the results presented here in terms of flavanol
446 association and penetration through the nucleus do not rule out the possibility that histones
447 may be a target for EGCG, catechin and epicatechin. Solution phase ultrafast structure and
448 dynamics studies such as time resolved infra-red (IR) or time resolved 2-dimensional IR
449 will be needed to probe the origin of the bi-exponential lifetimes, which differed between
450 the three flavanols. Such time resolved spectroscopic techniques will indicate the functional
451 groups responsible for the fast dynamics that differ amongst these flavanols.

452

453 3.7. *Future prospects*

454 Given the recent discoveries identifying that flavanols may well be involved in epigenetic
455 changes, highly sensitive techniques will be needed to trace their uptake and trafficking at
456 the sub-cellular and sub-nuclear level and at physiologically relevant concentrations. Our
457 results suggest that not all flavanols will interact via the same molecular mechanism and
458 this will require new techniques with sufficient specificity and sensitivity. New
459 developments in fluorescence lifetime imaging techniques and ultra-fast spectroscopy, as
460 demonstrated here, may hold the key and pave the way for studying their functions and
461 synthesis in plant cells. The trafficking, uptake and subcellular localisation of flavanols is
462 of acute interest also for current research on tannin synthesis in plants [55]. Unravelling this
463 last hurdle of flavonoid biosynthesis, storage and release would facilitate the development
464 of new plant varieties with tannin compositions that can offer enhanced biological activities
465 for nutrition and health [11].

466 Such analytical developments will facilitate new types of biological experiments that can
467 test how these compounds, when present in plant foods, can impact on mammalian cells
468 and health. Although FLIM is a new technique to both mammalian and plant cell biologists
469 alike, its application is growing rapidly [23-26,28], particularly in protein-protein
470 interactions that involve energy transfer processes. However, this is the first study to report
471 FLIM for other plant components and as the technique becomes more readily available, its
472 impact can only grow. This study has shown that relatively small changes in flavanol
473 structures (EGCG *versus* catechin or epicatechin; Fig. 1) lead to measurable changes in
474 lifetime behaviour in the free and bound states. As plants synthesise several types of
475 flavonoids, that vary in oxidation and substitution patterns [1], it is expected that other

476 flavonoid compounds will be detectable using different combinations of excitation and
477 emission wavelengths.

478

479 **4. Conclusions**

480 In conclusion, 2-photon excitation at 585 and 630 nm has enabled for the first time the
481 measurement of fluorescence lifetimes from three flavanols, catechin, epicatechin and
482 EGCG, in solution and *in vivo*. Lifetimes ranging from <45 ps to 1 ns in solution have been
483 determined. *In vivo* experiments with onion cells demonstrated that tryptophan and
484 quercetin have sufficiently low absorbance at 630 nm and this allowed the detection of
485 externally added and endogenous flavanols within *Allium cepa* and *Taxus baccata* cells.
486 Interestingly, fluorescence decay curves of catechin and EGCG differed markedly both in
487 solution and when bound at the nucleus. This fact could be used in the future for selectively
488 tracing the different flavanols *in vivo*. Furthermore, this work demonstrates how the
489 application of fluorescence lifetime technology may be used to investigate the way
490 flavanols interact with individual cellular components. We also conclude that flavanols are
491 absorbed by cell nuclei and this provides new research challenges with regard to their
492 intracellular functions.

493

494 Semi-quantitative measurements revealed that the relative ratios of EGCG concentrations in
495 perinucleolar organiser regions : nucleus : cytoplasm were approximately 100:10:1.

496 Moreover, 3-D FLIM showed that externally added EGCG penetrated the whole nucleus of
497 onion cells and was not just absorbed on the surface. The FLIM technique described here
498 proved therefore a significant advance to DMACA staining and is capable of providing

499 quantitative biophysical information to probe the intra-cellular functions of flavanols such
500 as EGCG, which is the major flavanol of green tea.

501

502 **Acknowledgements**

503 We are grateful to the Science and Technology Facilities Council for facility access time
504 and financial support (No 81072) and to Professor R.H. Bisby, Salford University, for
505 helpful discussions.

506

507 **References**

- 508 [1] J.A.M. Kyle, G.G. Duthie, in: Ø.M. Anderson, K.R. Markham (Eds.), *Flavonoids:*
509 *Chemistry, Biochemistry and Applications*, CRC Press, Boca Raton, 2006, pp. 219-
510 255.
- 511 [2] P.J. Hernes, J.I. Hedges, *Geochim. Cosmochim. Acta.* 68 (2004) 1293–1307.
- 512 [3] R.M. Hackman, J.A. Polagruto, Q.Y. Zhu, B. Sun, H. Fujii, C.L. Keen, *Phytochem.*
513 *Rev.* 7 (2008) 195-208.
- 514 [4] J.D. Lambert, R.J. Elias, *Arch. Biochem. Biophys.* 501 (2010) 65-72.
- 515 [5] S. Sang, J.D. Lambert, C.S. Yang, *J. Sci. Food Agric.* 86 (2006) 2256-2265.
- 516 [6] G. Williamson, C. Manach, *Am. J. Clin. Nutr.* 81 (suppl) (2005) 243S–55S.
- 517 [7] W.J.L. Lee, J.-Y. Sim, B.T. Zhu, *Mol. Pharmacol.* 68 (2005) 1018-1030.
- 518 [8] M. Clifford, J.E. Brown, in: Ø.M. Anderson, K.R. Markham (Eds.), *Flavonoids:*
519 *Chemistry, Biochemistry and Applications*, CRC Press, Boca Raton, 2006, pp. 319-
520 370.
- 521 [9] B. Holst, G. Williamson, *Curr. Opin. Biotechnol.* 18 (2008) 73-82.

- 522 [10] I. Hernández, L. Alegre, F. Van Breusegem, S. Munné-Bosch, *Trends Plant Sci.* 14
523 (2009) 125-132.
- 524 [11] I. Mueller-Harvey, *J. Sci. Food Agric.* 86 (2006) 2010-2037.
- 525 [12] J.D. Lambert, J. Hong, G.-Y. Yang, J. Liao, C.S. Yang, *Am. J. Clin. Nutr.* 81
526 (suppl.) (2005) 284S-291S.
- 527 [13] W. Feucht, H. Dithmar, J. Polster, *Internat. J. Mol. Sci.* 8 (2007) 635-650.
- 528 [14] W. Feucht, D. Treutter, H. Dithmar, J. Polster, *Tree Physiol.* 28 (2008) 1783-1791.
- 529 [15] W. Feucht, H. Dithmar, J. Polster, *J. Bot.* (2009) Article ID 842869 ([doi:
530 10.1155/2009/842869](https://doi.org/10.1155/2009/842869))
- 531 [16] J. Polster, H. Dithmar, W. Feucht, *Biol. Chem.* 384 (2003) 997-1006.
- 532 [17] J. Bauer, K. Neubauer, H. Dithmar, J. Polster, W. Feucht, *Adv. Food Sci.* 31 (2009)
533 82-88.
- 534 [18] J. Polster, H. Dithmar, R. Burgemeister, G. Friedemann, W. Feucht, *Physiol. Plant.*
535 128 (2006) 163-174.
- 536 [19] D. Treutter, *J. Chromatogr.* 467 (1989) 185-193.
- 537 [20] A.-P. Nifli, P.A. Theodoropoulos, S. Munier, C. Castagnino, E. Roussakis, H.E.
538 Katerinopoulos, J. Vercauteren, E. Castanas, *J. Agric. Food Chem.* 55 (2007) 2873-
539 2878.
- 540 [21] K. Suhling, P.M. French, D. Phillips, *Photochem. Photobiol. Sci.* 4 (2005) 13-22.
- 541 [22] E.B. van Munster, T.W.J. Gadella, *Adv. Biochem. Eng. Biotechnol.* 95 (2005) 143-
542 175.
- 543 [23] S.W. Botchway, A.W. Parker, R.H. Bisby, A.G. Crisostomo, *Microsc. Res. Tech.*
544 71 (2008) 267-273.

- 545 [24] A. Osterrieder, C.M. Carvalho, M. Latijnhouwers, J.N. Johansen, C. Stubbs, S.
546 Botchway, C. Hawes, *Traffic*. 10 (2009) 1-13.
- 547 [25] R.H. Bisby, S.W. Botchway, A.G. Crisostomo, J. Karolin, A.W. Parker, L.
548 Schröder, *Spectroscopy* 24 (2010) 137-142.
- 549 [26] S.W. Botchway, M. Charnley, J.W. Haycock, A.W. Parker, D.L. Rochester, J.A.
550 Weinstein, J.A.G. Williams, *PNAS*, 105 (2008) 16071-16076.
- 551 [27] P.T.C. So, C.Y. Dong, B.R. Masters, K.M. Berland, *Annu. Rev. Biomed. Eng.* 2
552 (2000) 399-429.
- 553 [28] I. Sparkes, N. Tolley, I. Aller, J. Svozil, A. Osterrieder, S. Botchway, C. Mueller, L.
554 Frigerio, C. Hawes, *Plant Cell* 22 (2010) 1333-1343.
- 555 [29] A. Rajavelu, Z. Tulyasheva, R. Jaiswal, A. Jeltsch, N. Kuhnert, *BMC Biochemistry*
556 12:16 (2011) [Doi:10.1186/1471-2091-12-16](https://doi.org/10.1186/1471-2091-12-16).
- 557 [30] W. Feucht, J. Polster, *Z. Naturforsch.* 56c (2001) 479-481.
- 558 [31] J.R. Lakowicz, *Principles of Fluorescence Spectroscopy*, fourth ed., Springer, New
559 York, 2006.
- 560 [32] D.F. Eaton, *Pure Appl. Chem.* 60 (1988) 1107-1114.
- 561 [33] Website: <http://omlc.ogi.edu/spectra/PhotochemCAD/html/tryptophan.html>
- 562 [34] S. Sang, M.-J. Lee, Z. Hou, C.-T. Ho, C.S. Yang, *J. Agric. Food Chem.* 53 (2005)
563 9478-9484.
- 564 [35] N.P. Slabbert, *Tetrahedron* 33 (1977) 821-824.
- 565 [36] M.A. Soobrattee, V.S. Neergheen, A. Luximon-Ramma, O.I. Aruoma, T. Bahorun,
566 *Mutation Res.* 579 (2005) 200-213.

- 567 [37] A.V. Probst, P.F. Fransz, J. Pazkowski, O. Mittelsten-Scheid, *Plant J.* 33 (2003)
568 743-749.
- 569 [38] D. Hernandez-Verdun, *J. Cell Sci.* 99 (1991) 465-471.
- 570 [39] F.L. Tobiason, R.W. Hemingway, G. Vergoten, *Basic Life Sci.* 66 (1999) 527-544.
- 571 [40] K.O., Chu, C.C. Wang, C.Y. Chu, K.W. Choy, C.P. Pang, M.S. Rogers, *Hum.*
572 *Reprod.* 22 (2007) 280-287.
- 573 [41] C.D. Kanakis, P.A. Tarantilis, M.G. Polissiou, S. Diamantoglou, H.A. Tajmir-Riahi,
574 *Cell Biochem. Biophys.* 49 (2007) 29-36.
- 575 [42] W. Feucht, H. Dithmar, J. Polster, *Plant Biol.* 6 (2004) 696-701.
- 576 [43] M.B. Inoue, M. Inoue, Q. Fernando, S. Valcic, B.N. Timmermann, *J. Inorg.*
577 *Biochem.* 88 (2002) 7-13.
- 578 [44] W.A. Peer, D.E. Brown, B.W. Tague, G.K. Muday, L. Taiz, A.S. Murphy, *Plant*
579 *Physiol.* 126 (2001) 536-548.
- 580 [45] D.E. Saslowsky, U. Warek, B.S.J. Winkel, *J. Biol. Chem.* 280 (2005) 23735-23740.
- 581 [46] H.O. Gutzeit, Y. Henker, B. Kind, A. Franz, *Biochem. Biophys. Res. Commun.* 318
582 (2004) 490-495.
- 583 [47] J. Grandmaison, R. Ibrahim, *J. Plant Physiol.* 147 (1996) 653-660.
- 584 [48] M.Z. Fang, Y. Wang, N. Ai, Z. Hou, Y. Sun, H. Lu, W. Welsh, C.S. Yang, *Cancer*
585 *Res.* 63 (2003) 7563-7570.
- 586 [49] T.M. Ehrman, D.J. Barlow, P.J. Hyland, *J. Chem. Inf. Model* 47 (2007) 254-263.
- 587 [50] K.-C. Choi, M.G. Jung, Y.-H. Lee, J.C. Yoon, S.H. Kwon, H.-B. Kang, M.-J. Kim,
588 J.-H. Cha, Y.J. Kim, W.J. Jun, J.M. Lee, H.-G. Yoon, *Cancer Res.* 69 (2009) 583-
589 592.

- 590 [51] M. Glei, B.L. Pool-Zobel, *Toxicol. in Vitro* 20 (2005) 295-300.
- 591 [52] L. Guo, L.H. Wang, B. Sun, J.Y. Yang, Y.Q. Zhao, Y.X. Dong, M.I. Spranger, C.F.
592 Wu, *J. Agric. Food Chem.* 55 (2007) 5881-5891.
- 593 [53] H. Yamada, H. Sugimura, T. Tsuneyoshi, *J. Food Agric. Environ.* 3 (2005) 73-76.
- 594 [54] J. Ordovás, C.E. Smith, *Nature Rev. Cardiol.* 7 (2010) 510-519.
- 595 [55] J. Zhao, Y. Pang, R.A. Dixon, *Plant Physiol.* 153 (2010) 437-443.
- 596

597 **Legend to Figures**

598

599 **Fig. 1:**

600 Structures of three flavanols, catechin (**1**), epicatechin (**2**), and epigallocatechin gallate (**3**),
601 and one flavonol, quercetin (**4**) (*note*: A, B, C denote the flavonoid rings).

602

603 **Fig. 2:**

604 The Jablonski diagramme depicting the energy levels of a molecule. S_0 represents the
605 ground singlet states, S_1 , S_2 the excited singlet states; T_1 the triplet excited states. Electronic
606 levels are subdivided into vibrational levels ($v_1, v_2 \dots v_n$). IC indicates internal conversion,
607 $k_{\text{fluorescence}}$: rate of fluorescence leading from S_1 ($v_1 = 0$) to S_0 (v_1 or v_n), k_{IVR} : intramolecular
608 vibrational relaxation, k_{ISC} : rate of intersystem crossing and k_{quench} : rate of reaction with
609 other molecules, chemical or energy transfer.

610

611 **Fig. 3:**

612 Time course of fluorescence lifetimes (ns) of catechin (2 mM) in 0.1 M phosphate buffer in
613 air or nitrogen atmospheres at pH 5.8, 7.1 and 8.2 ($\lambda_{\text{ex}} = 585$ nm).

614

615 **Fig. 4:**

616 Fluorescence decay curves of catechin, epicatechin and epigallocatechin gallate (EGCG)
617 solutions (2 mM) in 0.1 M phosphate buffer at pH 8.1 ($\lambda_{\text{ex}} = 585$ nm).

618

619 **Fig. 5:**

620 Fluorescence lifetime images ($\lambda_{\text{ex}} = 630 \text{ nm}$) of a cell from an onion epidermis soaked in 1
621 mM aqueous solutions of a) catechin ($\tau_1 = 0.4 \text{ ns}$ (82%), $\tau_2 = 2.6 \text{ ns}$ (18%)), b)
622 epigallocatechin gallate ($\tau = 0.2 \text{ ns}$) and c) control in water without added flavanol. Image
623 (A) shows a steady state image of the total emission lifetimes and image (B) shows the
624 analysed fluorescence excited state map. The distribution of fluorescence lifetimes in (B) is
625 illustrated in image (C), where the vertical axis represents the frequency and the horizontal
626 axis represents lifetime in pico-seconds. (*Note*: control nucleus shows hardly any
627 fluorescence in Fig. 5c).

628

629 **Supporting information**

630 Additional Supporting Information may be found in the online version of this article:

631 **Supplementary Table:** Fluorescence lifetimes (ns) of flavanols in the presence of different
632 histones (Tris buffers, pH 7 and 8). Pre-exponential factors are shown in brackets.

633

634 **Fig. S1.** UV-Vis spectra of catechin, epicatechin and epigallocatechin gallate recorded from
635 200 to 595 nm.

636

637 **Video Clip S1.** 3D stack of multiphoton excited ($\lambda_{\text{ex}} = 630 \text{ nm}$) fluorescence image from an
638 onion cell epidermis soaked in a 1mM aqueous solution of epigallocatechin gallate. Images
639 were recorded at 0.5 - 2.0 μm slices.

640

641 Please note: Wiley Blackwell are not responsible for the content or functionality of any
642 supporting materials supplied by the authors. Any queries (other than missing material)
643 should be directed to the corresponding author for the article.

644
645

646 **Table 1**

647 Fluorescence quantum yields of catechin, epicatechin and epigallocatechin gallate (EGCG)
648 in methanol at 37 °C.

649

Compound	Quantum yield^a
Catechin	0.018
Epicatechin	0.015
EGCG	0.003

650

651 ^a Estimated accuracy = ±16%

652

653 **Table 2**

654 Fluorescence lifetimes (ns) and pre-exponential factors (A_1 and A_2) of externally added
 655 flavanols, which were absorbed by onion epidermis, and endogenous flavanols in *Taxus*
 656 *baccata* male cones (\pm standard deviations).
 657

Sample	τ_1 (ns)	A_1 %	τ_2 (ns)	A_2 %
Onion epidermis:				
control in water	0.84 ^a	100		
Onion epidermis:				
+ catechin	0.5 \pm 0.04	77.5 \pm 6.92	2.7 \pm 0.19	22.5 \pm 6.92
+ epigallocatechin gallate (EGCG)	0.25 \pm 0.05	99.2 \pm 1.13		
<i>Taxus baccata</i> male cones:				
in water	0.2 \pm 0.03	93.4 \pm 6.46	0.5 \pm 0.2	6.6 \pm 6.46

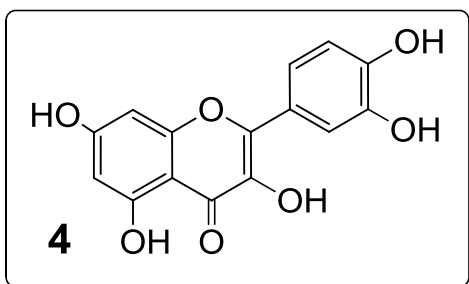
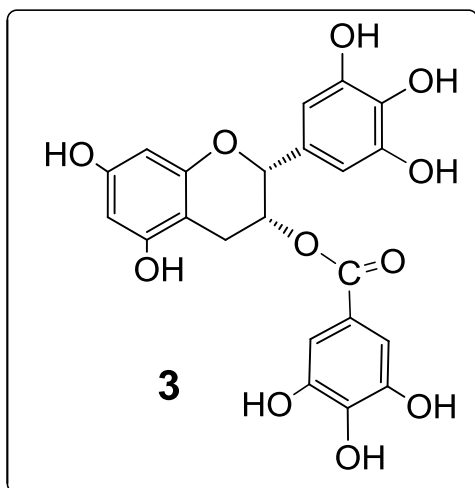
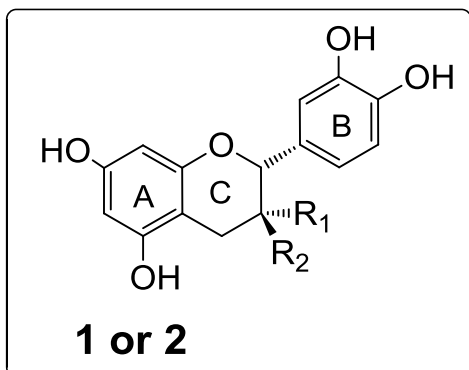
658

659 ^a The control had a very low photon count in the absence of externally added flavanols and
 660 the data were quite noisy (see Fig. 5c), therefore it was not possible to obtain a standard
 661 deviation of the background lifetime.

662

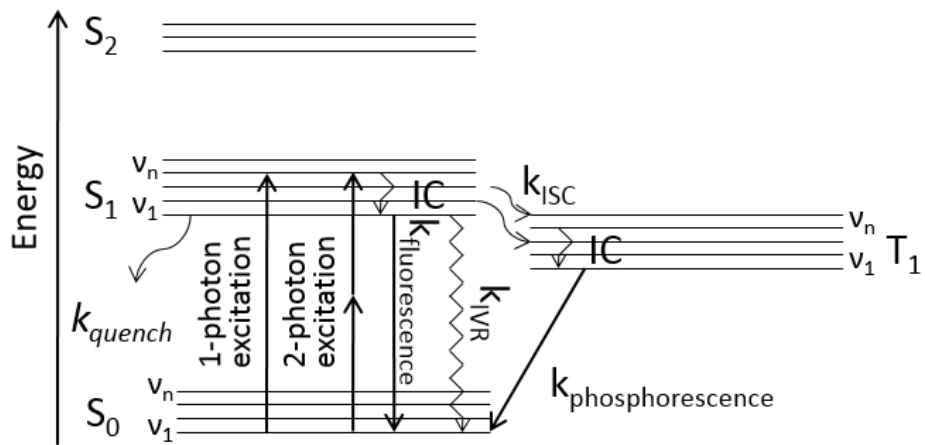
663

664 **Figure 1:**
665

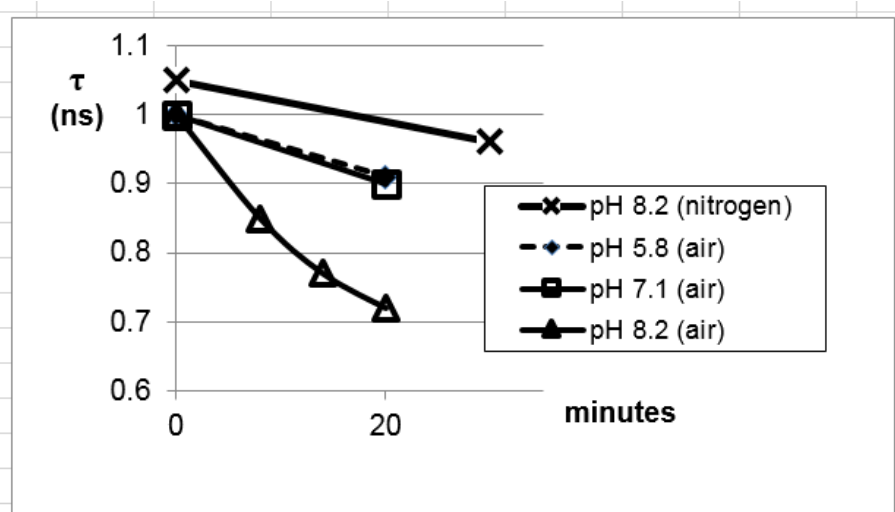


666
667
668

669 Fig 2
670

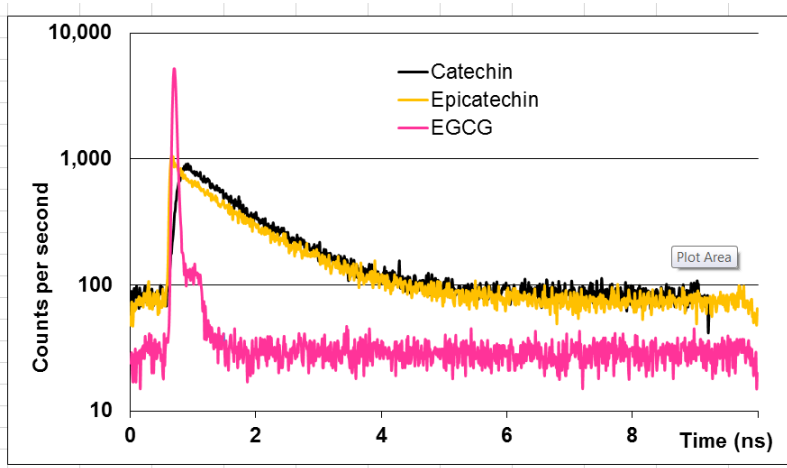


671
672
673 Fig 3
674



675
676

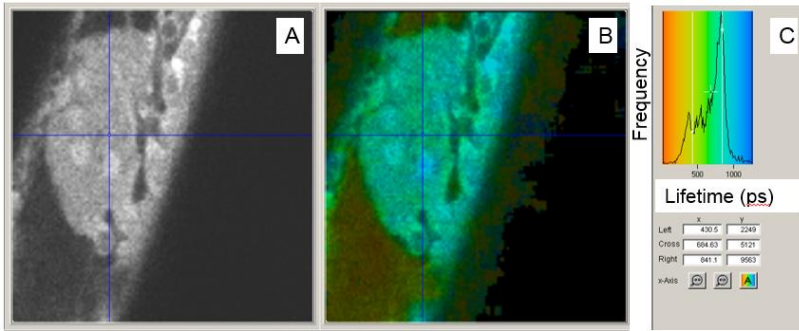
677 Fig 4



678

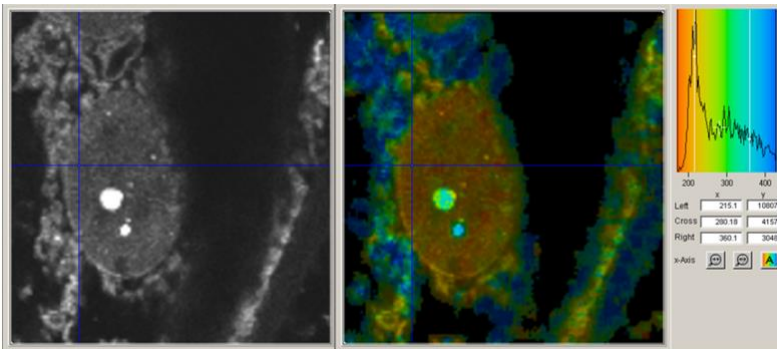
679

680 Fig 5a



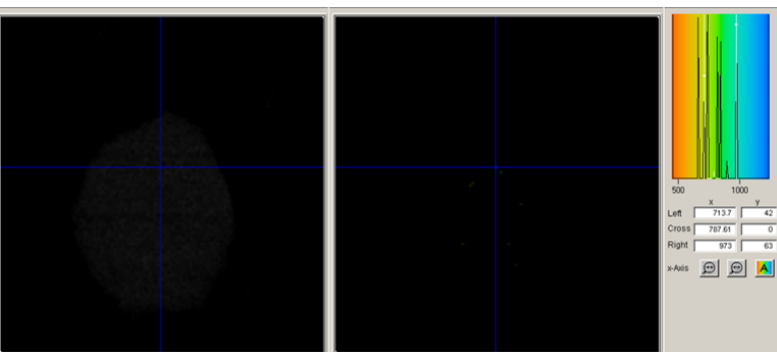
681

682 Fig 5 b



683

684 Fig 5c



685

686

687

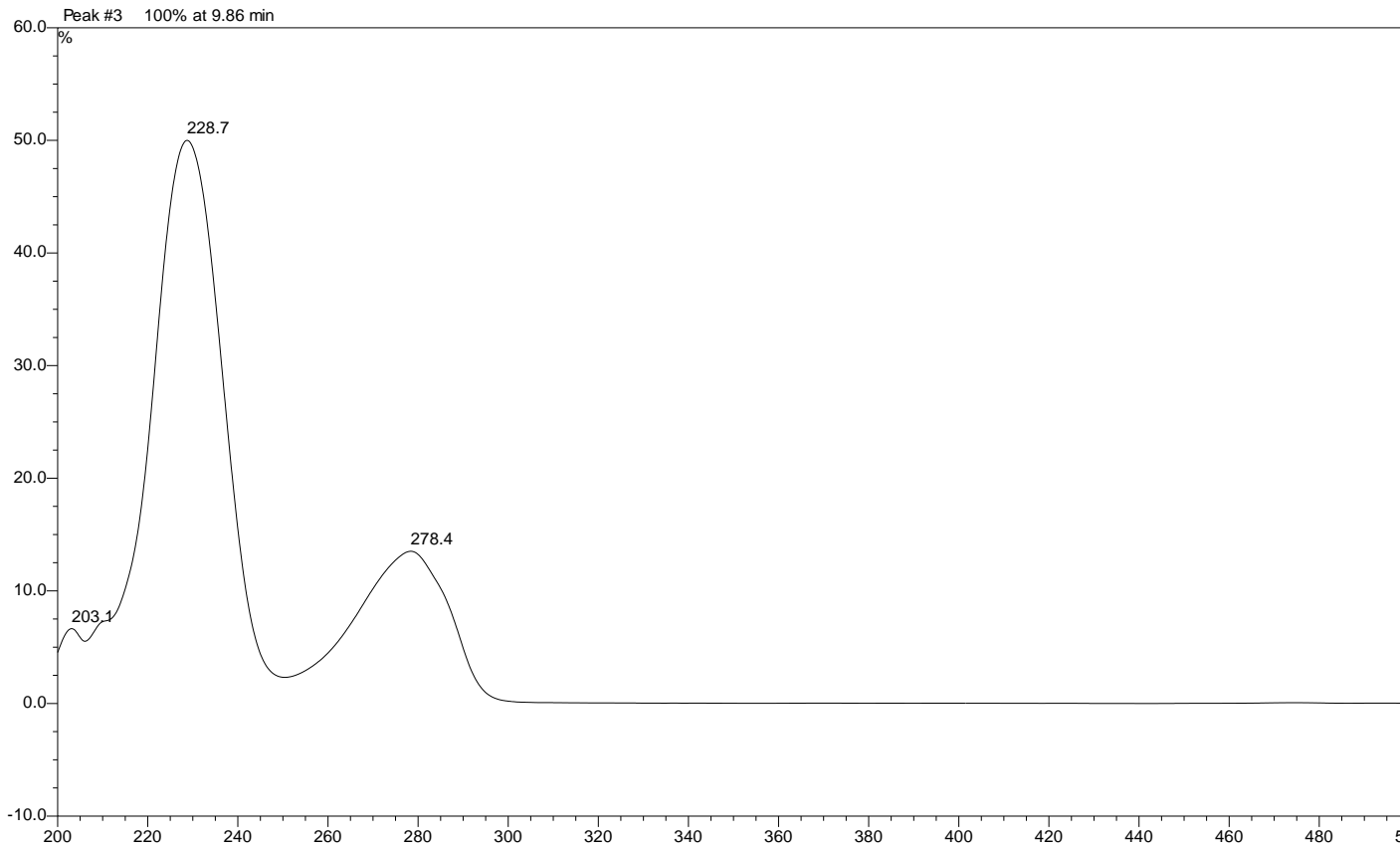
688 Fig S1

689 **Figure S1:** UV-Vis spectra of catechin, epicatechin and epigallocatechin
690 gallate recorded from 200 to 595 nm.

691

692 **Catechin**

693



694

695

696

697

698

699

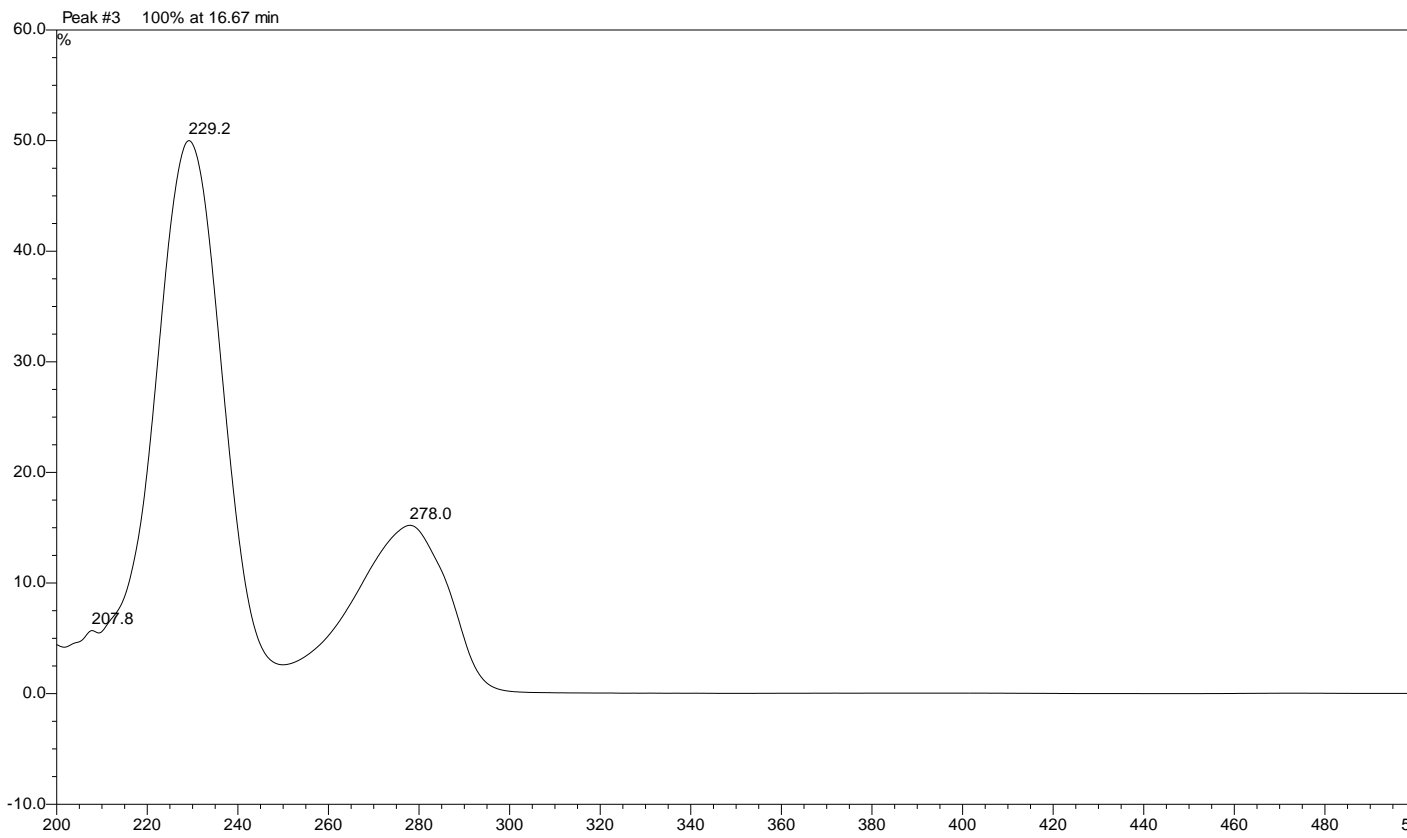
700

701

702

703

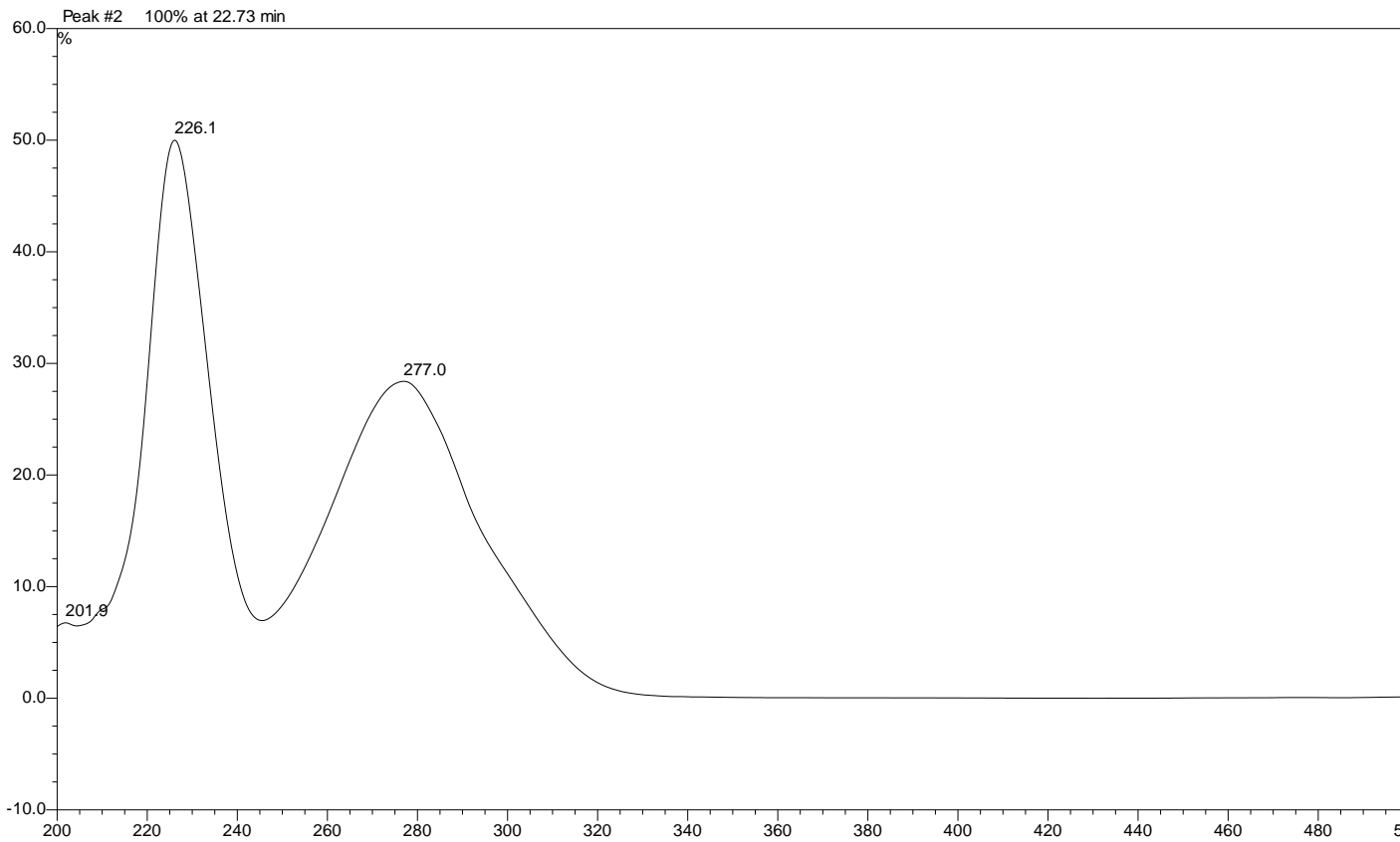
704 **Epicatechin**
705



706
707
708
709
710
711
712
713
714
715

716 **Epicatechin gallate**

717



718
719

720 Supplementary **Table**

721 Fluorescence lifetimes (ns) of flavanols in the presence of different histones (Tris buffers, pH 7 and 8). Pre-exponential factors

722 are shown in brackets.

	1 mM Flavanol				2 mM Flavanol			
	pH 7		pH 8		pH 7		pH 8 ^b	
	τ_1^a	τ_2	τ_1	τ_2	τ_1	τ_2	τ_1	τ_2
(+)-Catechin^b								
+ Sigma histone	0.9 (75%)	1.9 (25%)	0.9 (92%)	2.5 (8%)	1.1 (82%)	1.7 (18%)	1.1 (80%)	1.9 (20%)
+ Histone sulphate	1.1 (95%)	4.0 (5%)	0.9 (75%)	2.0 (25%)	1.1 (88%)	2.1 (12%)	1.1 (88%)	2.0 (12%)
+ Roche histone	1.0 (96%)	3.5 (4%)	0.9 (80%)	2.7 (20%)	0.8 (86%)	2.5 (14%)	1.1 (93%)	3.2 (7%)
(-)-Epicatechin^b								
+ Sigma histone	0.8 (75%)	2.0 (25%)	0.9 (90%)	2.5 (10%)	1.1 (85%)	1.8 (15%)	1.0 (86%)	2.0 (14%)
+ Histone sulphate	nd ^c	nd	nd	nd	1.1 (87%)	1.9 (13%)	1.0 (84%)	1.9 (16%)
+ Roche histone	1.0 (92%)	2.8 (10%)	0.9 (80%)	2.3 (20%)	1.1 (90%)	3.1 (10%)	1.0 (90%)	2.7 (10%)
Average	0.9	2.4	0.9	2.3	1.1	2.3	1.1	2.4

723 ^a Experimental error is ± 50 ps; ^b For comparison, lifetime measurements in 0.1 M phosphate buffer at pH 8.1 gave $\tau = 1.0$ ns for724 catechin and $\tau_1 = 1.1$ (72%) and $\tau_2 = 0.1$ ns (28%) for epicatechin (note: Due to the poor signal-to-noise at longer times the errors725 are significantly larger for the second lifetime (τ_2) and the pre-exponential factors of less than 10% may be due to a fluorescence726 contribution from impurities); ^c nd = not determined.